

Device reliability study of high gate electric field effects in AlGaIn/GaN high electron mobility transistors using low frequency noise spectroscopy

Hemant Rao^{a)} and Gijs Bosman

Department of Electrical and Computer Engineering, University of Florida, Gainesville, Florida 32611, USA

(Received 28 January 2010; accepted 12 July 2010; published online 7 September 2010)

Low frequency noise characteristics of gate and drain currents are investigated for prestressed and poststressed AlGaIn/GaN high electron mobility transistors. High reverse bias voltage stresses on the gate stack changes both drain and gate current noise. A temporary increase in drain current noise was observed during stress which recovered to prestress level a few weeks later. This is explained via a positive and negative threshold voltage shift due to electron trapping under the gate during and after stress, respectively. On the other hand, gate current noise shows a permanent increase after the stress which is not seen to recover once the stress is removed. It is proposed that new defect states are created below the metal AlGaIn layer of the gate edges which leads to a permanent degradation of gate current noise. © 2010 American Institute of Physics. [doi:10.1063/1.3475991]

I. INTRODUCTION

AlGaIn/GaN based transistor structures exhibit strong piezoelectric and spontaneous polarization fields which produce high sheet carrier densities at the heterointerface.¹ These polarization fields are sufficiently large to induce high carrier densities without intentional doping thereby reducing ionized impurity scattering leading to high mobility in the channel. This feature along with wide band gap of nitride semiconductors makes AlGaIn/GaN heterostructure transistors very promising for high frequency and high power applications. Reliability is a crucial requirement for increased commercial application of this technology.² Many prominent degradation mechanisms have been identified by various groups which cause temporary and permanent changes in the electronic and material structures of the device.^{3–5} Figure 1 shows a classification of prominent degradation mechanisms in these devices as a function of physical effect. Except polarization most of these effects have been well studied in other III-V high electron mobility transistors (HEMTs) and are relevant for nitride transistors as well. Lattice mismatch induced strain in the AlGaIn barrier via inverse-piezoelectric effect has been identified as one of the key cause of degradation at high electric fields under the gate stack.⁶ rf devices experience high gate reverse bias during normal operations which cause large vertical fields below the gate. Therefore, it is important to probe this effect in more detail.

Low frequency noise is known to be an extremely sensitive tool for studying reliability and changes in electronic structure due to degradation.^{7,8} A few reliability studies have been performed in these devices using drain current noise to understand changes in the channel region.^{9–12} Most of these groups have concluded that off-state stress does not seem to cause major changes in drain noise. This work, on the other hand, demonstrates that interesting things are happening right below the gate stack which does not seem to be affecting the channel and thereby drain noise. To gain a detailed

understanding, a simultaneous measurement of gate and drain current noise is necessary to isolate degradation in the gate stack and/or the heterostructure interface.¹³ This paper demonstrates the results of dc and low frequency noise characterization of gate and drain currents in AlGaIn/GaN HEMTs which were stressed to high reverse gate biases with source and drain connected to ground. Noise and IV measurements were performed during and after stress in both frequency and time domain. Temporary and permanent changes in the electronic structure of the device are delineated and physical locations of degradation are identified.

II. DEVICE DESCRIPTION AND EXPERIMENTAL SETUP

The devices under study have an $\text{Al}_{0.26}\text{Ga}_{0.74}\text{N}/\text{GaN}$ structure grown on high resistivity Si substrate by metal organic chemical vapor deposition. A Schottky gate contact is made of Ni/Au and Ohmic contacts for drain and source are made of Ti/Al. The transistors have SiN passivation and a single source field plate. The devices are also packaged to avoid any ambient optical instability to affect electrical measurements. More details can be found in a previous work.¹³

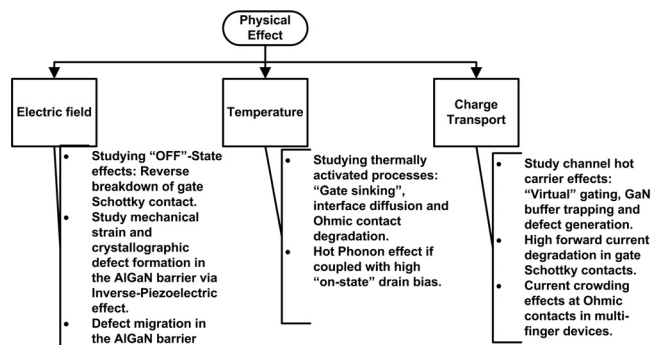


FIG. 1. Illustration of prominent failure mechanisms in AlGaIn/GaN HEMTs as a function of physical effects. This work limits its study to the electric field driven effects particularly in the "OFF" state.

^{a)}Electronic mail: phemantrao@ufl.edu.

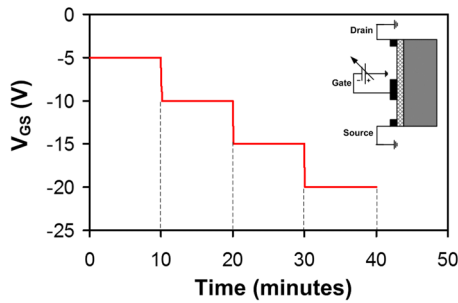


FIG. 2. (Color online) The solid line indicates the step-voltage stress from -5 to -20 V applied to the gate terminal where source and drain are connected to ground (biasing shown in the inset). The measurements are performed at the end of the 10 min stress period (indicated by dashed line) by measuring I_{DS} , I_{GS} vs V_{GS} , drain current noise, and gate current noise.

A characterization suite is developed for performing stress, dc, and noise measurements in an automated sequence. A semiconductor parameter analyzer HP4145B is configured for performing both electrical stress and IV measurements. Figure 2 shows the stress protocol and time instances when a measurement is performed. The gate is stressed by applying a stepped reverse bias from -5 to -20 V with -5 V increment for 10 min each. After each cycle, stress is stopped and dc transconductance, drain and gate current noise are measured. Both drain and gate dc currents are measured at low V_{DS} of 80 mV. Low frequency noise of gate and drain currents is measured at a constant V_{DS} and V_{GS} of 80 mV and -1.23 V, respectively, using a setup developed by the authors in a previous work.¹⁵ As will be shown later, threshold voltage itself changed during stress and the chosen value of gate voltage for measuring noise was found to be appropriate for keeping the device in strong inversion. It should be mentioned here that dc and noise measurements were carried out also several weeks after the stress was applied which was useful for isolating transient trapping and detrapping effects from permanent changes in the device electrical properties.

III. STRESS CHARACTERIZATION RESULTS

A. dc characterization

The focus of this work was to understand changes in the low frequency noise characteristics of the device which undergoes systematically applied electrical stress. Therefore, the dc parameters which were monitored during the stress were mainly chosen for convenience to extract the relevant noise figures. The noise measurements were conducted at low drain current and voltage levels which were significantly smaller than the stress conditions making the measurements electrically benign so as not to alter the device characteristics. The inset of Fig. 3(a) shows the measured drain current transfer characteristics before and after stress, respectively. A large positive shift can be seen in the threshold voltage which forces a drift in the transfer characteristics. The peak value of the transconductance (g_m) was found to be constant with an overall positive voltage shift before and after stress indicating that no major changes took place in the channel region. As mentioned earlier dc characterization was also carried out several weeks after the stress was removed to

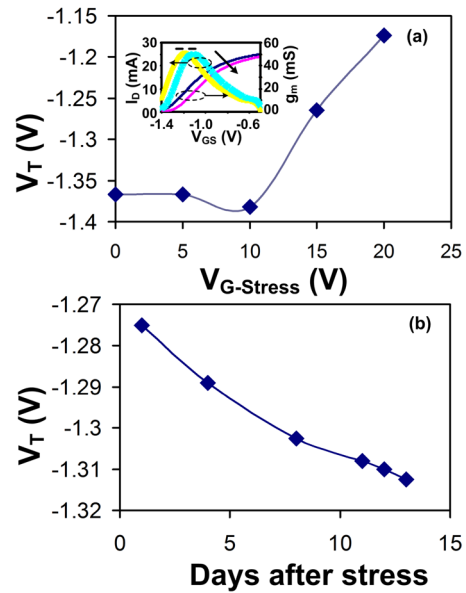


FIG. 3. (Color online) Top figure (a) shows the increase in threshold voltage during stress. The inset in (a) depicts the prestress and poststress drain current transfer (I_{DS} - V_{GS}) characteristics at $V_{DS}=80$ mV. The slow threshold voltage recovery is shown in bottom figure (b).

isolate transient trapping detrapping effects. Figures 3(a) and 3(b) show the changes in the threshold voltage of the device during and after stress, respectively. It can be clearly seen that a large positive V_T shift is induced during stress changing it from -1.36 to -1.17 V in a span of 40 min. This recovers back to prestress levels several days later. In subsequent sections it will be seen that drain current noise also changes in accordance with this large V_T shift due to a change in sheet carrier concentration in the channel. Gate leakage current was also measured simultaneously with drain current in the transfer characteristics. Figure 4 shows the evolution of gate leakage current during stress. It shows a constant decline and exhibits large relative fluctuations contributing to large gate current noise in the frequency domain.

B. Drain current noise characterization

Drain current noise is very sensitive to the defect states affecting charge transport in the channel and access regions making it an excellent indicator of the channel quality. Nor-

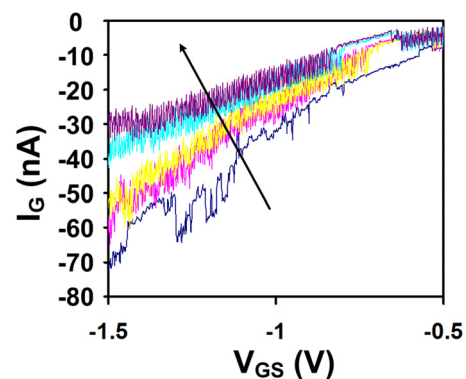


FIG. 4. (Color online) The evolution of the gate leakage current measured at $V_{DS}=80$ mV during stress is shown at each stress-step. An overall decrease is seen (indicated by the arrow) as stress is increased.

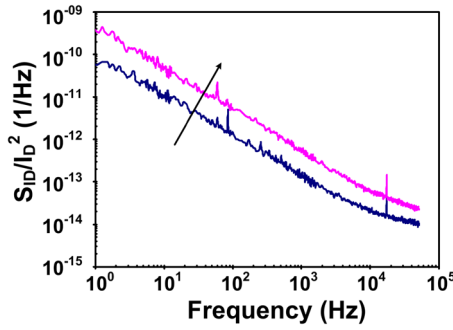


FIG. 5. (Color online) Normalized drain current spectra (S_{ID}/I_D^2) for prestress and poststress cases. An increase by a factor of 4 is seen indicated by the arrow. This increase was found to temporary and it fully recovered to its prestress levels a few weeks later as the dc threshold voltage recovered.

malized drain current noise was measured as a function of gate bias to identify the dominant noise sources from different parts of the channel. It was found that the gated part of the channel was the main source of drain current noise.¹³ A dc gate voltage of -1.23 V was chosen for noise measurement since both channel noise and resistance dominate in that region. Figure 5 shows the drain current noise before and after stress at the same dc bias level. An increase by a factor of 4 is visible in the spectra. It was observed that this increase was temporary and the noise recovered completely to its prestress levels a few weeks later. Hooke equation of the normalized drain current noise can be written as

$$\frac{S_{ID}}{I_D^2} \cong \frac{S_{RCH}}{R_{CH}^2} = \frac{\alpha_{CH}}{A_{CH}N_{CH}f}, \quad (1)$$

where S_{RCH} , R_{CH} , and A_{CH} represent the resistance noise, resistance of the gated part of the channel, and area of the channel, respectively. In the triode region at low drain voltages, the sheet carrier concentration in the channel (N_{CH}) is directly proportional to the gate overdrive voltage given by

$$N_{CH} = \frac{1}{q} C_{AlGaN} (V_{GS} - V_T), \quad (2)$$

where C_{AlGaN} is the capacitance per unit area of the AlGaIn layer. Assuming α_H remains the same and noise is measured at a constant V_{GS} . A change in V_T of around 0.2 V causes a change in the channel carriers which in turn changes S_{ID}/I_D^2 by a factor of around 4. This explains the noted shift in the drain current noise both during and after stress. Therefore, it can be concluded that the channel is immune to any degradation due to high gate reverse biases.

C. Gate current noise characterization

Figure 6 shows the prestress and poststress normalized gate current power spectra. An increase by a factor of 10 is seen in the spectra. On the other hand the dc gate leakage current measured at $V_{GS} = -1.23$ V increased only by a factor of 2. Initially it seemed that this was analogous to the drain noise increase which would recover once the stress was removed. It was found that this increase was permanent and no recovery could be obtained even several weeks later. Furthermore, it showed a temporal instability with Lorentzians

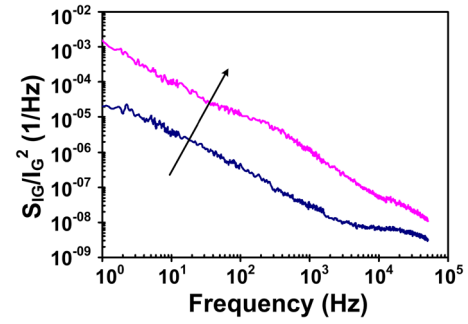


FIG. 6. (Color online) Normalized gate current noise (S_{IG}/I_G^2) for prestress and poststress cases. An increase by a factor of 10 can be seen (indicated by the arrow). This shift was found to be permanent and did not recover.

shifting positions in the frequency domain. Two level switching was also observed in the time domain with varying characteristic times. This phenomenon was observed in a previous work by the authors and can be linked to an electrical activation of mobile defect centers after stress.¹³ In order to get a better understanding of these changes a low temperature noise measurement was performed to reduce the temporal instability of the Lorentzians. The device was cooled to 77 K and noise was measured. Interestingly, in the triode region at $V_{DS} = 80$ mV a $1/f^2$ -type spectra was obtained but when the device was biased in saturation at $V_{DS} = 2$ V a large Lorentzian emerged in the gate noise spectra (Fig. 7). This same behavior was seen when the source and drain were swapped.

IV. DISCUSSION

In this part, a critical analysis of the physical origins of the results is performed. The results suggest that two dominant mechanisms are at play. First are the transient effects due to existing defects which affect dc device characteristics and drain current noise. Second are the permanent changes in the material structure which changes the gate current noise in a significant way. Earlier it was shown that threshold voltage shifted positively during stress and later recovered to prestress levels. The threshold voltage is typically determined by the gate metal semiconductor barrier height, band discontinuity at AlGaIn/GaN interface, polarization charges, and fixed defect states in the barrier.¹⁴ It was found that forward

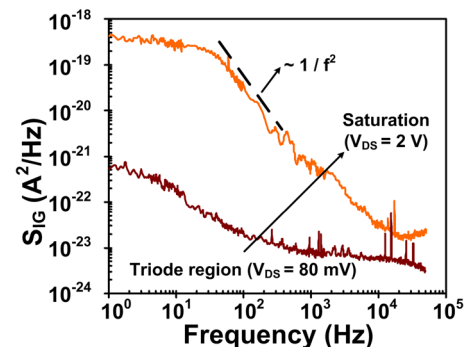


FIG. 7. (Color online) Gate current noise (S_{IG}) measured at 77 K for two dc biasing in triode region and saturation at a $V_{GS} = -1.23$ V. A drastic increase in noise is seen in saturation with a distinct Lorentzian at a corner frequency of 30 Hz.

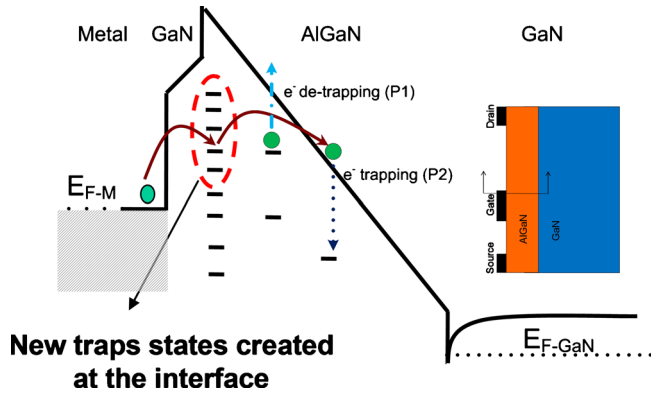


FIG. 8. (Color online) Conduction band diagram of the cross-section at the gate-drain edge (shown in the device structure on the right). Electrons tunneling in and out (shown in solid arrows) contribute to the increased dc gate leakage current and gate current noise. New trap states are created (indicated by dashed circle) in the AlGaN barrier which are above the metal Fermi level (E_{F-M}). P1 (dashed-dotted arrow) shows the detrapping of electrons from the existing traps which contribute to recovery of threshold voltage after stress. P2 (dotted arrow) shows the trapping of electrons which tunnel from the gate terminal during stress. They lead to an increase in the threshold voltage.

biasing of the gate to source-drain diode led to a faster recovery of threshold voltage to prestress levels. Studies performed on similar devices (GaN-on-Si) by other groups have shown that threshold voltage also recovers by optical excitation via UV light illumination with a frequency comparable to the band gap of the barrier.¹⁵ The band discontinuity and polarization charges would be invariant to both optical excitation and forward biasing of the gate-to-channel diode. Furthermore, a change in these parameters during stress would be permanent in nature and would be irreversible unlike what was observed. Therefore, it can be assumed that threshold voltage shift is due to the charging and discharging of fixed defect states in the AlGaN barrier. The exact physical distribution of the traps is unknown at this time, so if it is assumed that a fixed sheet charge is located in the AlGaN barrier near the channel, then the effective trap density can be deduced from the relation

$$\Delta V_T \cong \frac{Q_F}{C_i} = \frac{qN_T d_{\text{AlGaN}}}{\epsilon_{\text{AlGaN}}}. \quad (3)$$

A positive shift of 0.2 V corresponds to an effective trap density (N_T) of $5 \times 10^{11} \text{ cm}^{-2}$. This value is smaller than the typical polarization charges at the interfaces.¹⁶ It has been shown that in AlGaN/GaN HEMTs at high reverse gate voltages ($V_{GS} \ll V_T$) the electrons predominantly tunnel from the gate edges.¹⁶ Some of these electrons can get trapped in the existing defect states in the AlGaN layer which will cause an increase in the threshold voltage. This is shown in process P2 in Fig. 8. This event will also lead to a change in the potential profile in the AlGaN barrier. Charged defect states decrease the band bending which in turn increases the barrier-width as seen by the tunneling electrons from the gate metal. The tunneling probability of electrons will thereby decrease resulting in reduced gate leakage current. Both these effects were visible in the measurement results. When the stress is removed the trapped electrons beneath the gate slowly detrap which leads to a recovery of the threshold voltage. Shown in

process P1 in Fig. 8. Gate current noise results demonstrated that a permanent change took place in the environment seen by the electrons tunneling from gate to semiconductor. In a previous work it was noted that $1/f^\gamma$ component of the spectra is due to the trap state fluctuation at the metal semiconductor Schottky interface.¹³ Since it increased by a factor of 10 it can be concluded that near interface defect density increased at the metal semiconductor junction and additional trap states were created. Low temperature measurements pointed out that when the device was biased at $V_{DS}=2 \text{ V}$ where the dc drain current was saturated, the gate noise increased dramatically. The same measurement was performed when source and drain terminals were swapped and a similar increase was observed. In the former experiment the vertical fields at the gate-drain edge become larger than fields at the center. In the latter case, the vertical fields at the gate source edge become larger than fields at the center. This leads to an increase in tunneling probability at the edges and more electrons at the Fermi level of the metal can access the trap states in the AlGaN leading to discrete switching noise. It is proposed that during stress new trap states were generated in the AlGaN barrier beneath both the gate edges which are most probably located above the metal Fermi level. Although it has been shown that inverse-piezoelectric breakdown not only degrades the AlGaN barrier but also the channel region in the GaN buffer.⁶ The results presented in this work do show degradation of the AlGaN barrier but not the channel. This could be due to relatively low stress voltages used in this work and/or a smearing down of peak electric field due to source field plate. Also the degradation is below the onset of the “critical voltage” for major breakdown. This demonstrates that low frequency noise is an insightful tool to predict early degradation at relatively low stress levels which eventually leads to large performance degradation at higher voltages. This large degradation not only affects noise but also change the dc characteristics drastically.

V. SUMMARY

In conclusion, temporary and permanent degradation of device characteristics are identified in stressed AlGaN/GaN HEMTs. It is found that existing traps in the AlGaN barrier layer contribute to the threshold voltage instability and change the drain current noise. The dc characteristics of the device fully recover after several days. On the other hand, gate current noise shows a permanent change which does not recover once the stress is removed. It is proposed that new defect states were created at gate edges via inverse-piezoelectric effect below the so called “critical voltage.” The exact nature of these new defect states needs to be explored further possibly by studying the temperature dependence of low frequency noise. Finally, it has been shown that low frequency noise spectroscopy can give early indications to device failure before actual breakdown occurs thus, acting as a powerful reliability characterization tool.

ACKNOWLEDGMENTS

This work was supported by AFOSR MURI (Grant No. FA9550-08-1-0264).

- ¹O. Ambacher, B. Foutz, J. Smart, J. R. Shealy, N. G. Weimann, K. Chu, M. Murphy, A. J. Sierakowski, W. J. Schaff, L. F. Eastman, R. Dimitrov, A. Mitchell, and M. Stutzmann, *J. Appl. Phys.* **87**, 334 (2000).
- ²G. Meneghesso, G. Verzellesi, F. Danesin, F. Rampazzo, F. Zanon, A. Tazzoli, M. Meneghini, and E. Zanoni, *IEEE Trans. Device Mater. Reliab.* **8**, 332 (2008).
- ³R. Vetry, N. Q. Zhang, S. Keller, and U. K. Mishra, *IEEE Trans. Electron Devices* **48**, 560 (2001).
- ⁴M. Faqir, G. Verzellesi, G. Meneghesso, E. Zanoni, and F. Fantini, *IEEE Trans. Electron Devices* **55**, 1592 (2008).
- ⁵G. Meneghesso, F. Rampazzo, P. Kordos, G. Verzellesi, and E. Zanoni, *IEEE Trans. Electron Devices* **53**, 2932 (2006).
- ⁶J. Joh and J. A. Del Alamo, *IEEE Electron Device Lett.* **29**, 287 (2008).
- ⁷L. K. J. Vandamme, *IEEE Trans. Electron Devices* **41**, 2176 (1994).
- ⁸E. Simoen and C. Claeys, *Semicond. Sci. Technol.* **14**, R61 (1999).
- ⁹C. Sury, A. Curutchet, N. Malbert, and N. Labat, in *Noise and Fluctuations: 20th International Conference on Noise and Fluctuations (ICNF-2009)*, edited by M. Macucci and G. Basso (AIP, Pisa, Italy, 2009), pp. 625–628.
- ¹⁰A. Curutchet, N. Malbert, N. Labat, A. Touboul, C. Gaquière, A. Minko, and M. Uren, *Microelectron. Reliab.* **43**, 1713 (2003).
- ¹¹D. K. Sahoo, R. K. Lal, H. Kim, V. Tilak, and L. F. Eastman, *IEEE Trans. Electron Devices* **50**, 1163 (2003).
- ¹²A. Sozza, C. Dua, E. Morvan, B. Grimber, and S. Delage, *Microelectron. Reliab.* **45**, 1617 (2005).
- ¹³H. Rao and G. Bosman, *J. Appl. Phys.* **106**, 103712 (2009).
- ¹⁴U. K. Mishra and J. Singh, *Semiconductor Device Physics and Design* (Springer, New York, 2007).
- ¹⁵S. Demirtas, J. Joh, and J. A. D. Alamo, *Microelectron. Reliab.* **50**, 758 (2010).
- ¹⁶D. M. Sathaiya and S. Karmalkar, *IEEE Trans. Electron Devices* **54**, 2614 (2007).